

# Total kinetic energy release in the fast neutron induced fission of actinide nuclei

Ashley Pica<sup>1</sup>, Alexander Chemey<sup>1</sup>, and Walter Loveland<sup>1</sup>

<sup>1</sup>Dept, of Chemistry, Oregon State University, Corvallis, OR 97331, USA

**Abstract.** The total kinetic energy (TKE) release in the fast neutron-induced fission of various actinide nuclei was measured for neutron energies for  $E_n=2.6-100$  MeV at the Weapons Neutron Research facility of the Los Alamos National Laboratory. The data are compared to the GEF model of the fission process. The variances of the TKE distributions appear to decrease with increasing  $Z$  and  $A$  of the fissioning systems.

## 1 Introduction

The largest part of the prompt energy release in fission (169.1 MeV out of 185.6 MeV for  $^{235}\text{U}(n_{th},f)$ ) is in the form of the total kinetic energy (TKE) of the fission fragments. Fission is a large scale collective motion of a few hundred nucleons and as such, is difficult to understand. The magnitude of the TKE release depends on the Coulomb forces between the nascent fragments at scission and the possible transfer of collective energy into either nucleonic excitation or fragment motion at scission. In this paper we describe the measurement of the TKE release in the fast neutron induced fission of  $^{232}\text{Th}$ ,  $^{235}\text{U}$  and  $^{237}\text{Np}$ . Some of these data have been published previously [1–3]. We comment on common features of these data and suggest directions for further research.

## 2 Experimental

The experimental arrangements for these measurements have been described in detail in [1–3]. The measurements were made at the Los Alamos National Laboratory using the Weapons Neutron Research Facility (WNR) at the Los Alamos Neutron Science Center (LANSCE). The measurements typically took 5-7 days. The targets were bombarded with “white spectrum” neutron beams generated from an unmoderated tungsten spallation source using the 800 MeV proton beam from the LANSCE linear accelerator. The experiment was located on the 15R beam line. The fast neutron beam intensities were  $10^5 - 10^6$  neutrons/s for  $E_n = 2-100$  MeV. The proton beam was pulsed allowing one to measure the time of flight of neutrons striking the actinide fission targets. The neutron energies were determined with an uncertainty of 4.7-5%. Because of the low beam intensities and relatively short measurement times, large solid angles had to be employed for the detection of any fission fragments produced.

The actinide targets were mounted at the center of an evacuated Al scattering chamber. Fission fragments from

the fast neutron-actinide reactions were detected by large arrays of Si PIN diode detectors. The actinide targets were  $\sim 195 \mu\text{g}/\text{cm}^2$  ( $^{232}\text{Th}$ ),  $\sim 175 \mu\text{g}/\text{cm}^2$  ( $^{235}\text{U}$ ), and  $34 \mu\text{g}/\text{cm}^2$  ( $^{237}\text{Np}$ ). The combination of similar measurement times and the thinner  $^{237}\text{Np}$  target lead to larger uncertainties in the  $^{237}\text{Np}$  measurements. The actinides were deposited on  $\sim 100 \mu\text{g}/\text{cm}^2$  C foil by vapor deposition [4].

We measured, on an event by event basis, the pulse heights of coincident fission fragments. To transform these pulse heights into energies, we corrected for the pulse height defect of our Si detectors and the energy loss of the fission fragments in the target and backing materials, iteratively. We used the 2E method to treat the data. In the 2E method, we corrected iteratively for (a) pre-equilibrium neutron emission (b) pre-fission neutron emission (c) the dependence of the post neutron emission on fragment mass and (d) the mean atomic number associated with each post neutron emission fragment. The pulse height defect is taken into account using the Schmitt procedure [5] and the energy losses in the target deposit and the target backing material are calculated using the Northcliffe-Schilling tables [6]. The GEF model [7] is used to estimate  $\nu_{pre-eq}$ ,  $\nu_{pre}$ ,  $\nu_{post}$ , and  $Z(A)$ .

To benchmark the experimental method, the TKE release in the  $^{235}\text{U}(n_{th},f)$  reaction was measured at the Oregon State University 1 MW TRIGA Reactor. The measurement was made using the same apparatus and target as in the LANSCE experiment. The thermal neutron-induced fission data at Oregon State University was analysed using the same methods and corrections as with the fast-neutron induced fission data, except  $\nu_{tot} = 2.5$  and  $\nu_{pre} = 0$ . The measured post-neutron emission TKE was  $169.8 \pm 0.4$  MeV. The deduced pre-fission TKE was  $170.7 \pm 0.4$  MeV. This result is consistent with previous measurements of  $171.9 \pm 1.4$  MeV [5],  $172.0 \pm 2.0$  MeV [8] and  $170.1 \pm 0.5$  MeV [9].

**The measurements of the TKE release in this work are thus absolute measurements with no normalizations to theory or other measurements.**

### 3 Data

#### 3.1 $^{232}\text{Th}(n,f)$

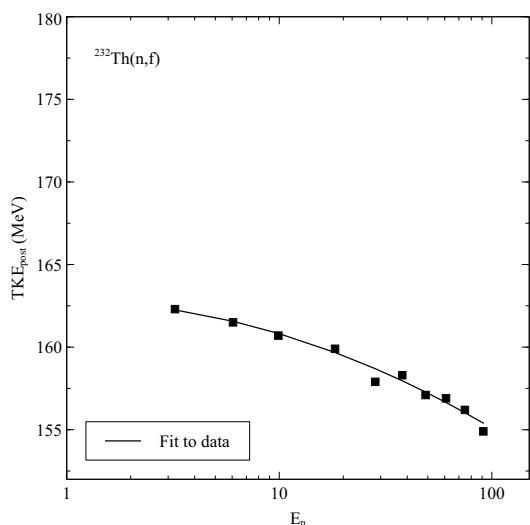


**Figure 1.** The average post-fission TKE measured for the  $^{232}\text{Th}(n,f)$  reaction as a function of neutron energy.

In Figure 1, we show the mean post-fission TKE release for the fast neutron induced fission of  $^{232}\text{Th}$  for the energy range from 3-91 MeV. For this energy range, the mean total kinetic energy decreases non-linearly from  $162.3 \pm 0.3$  MeV to  $154.9 \pm 0.3$  MeV. A polynomial fit was made to these data. The resulting polynomial is  $\text{TKE}_{post} \text{ (MeV)} = 162.8 - 0.1884 \log_{10} E_n - 1.866 (\log_{10} E_n)^2$ .

#### 3.2 $^{235}\text{U}(n,f)$

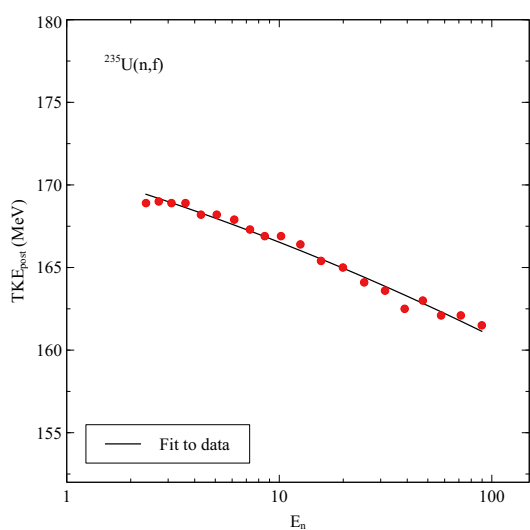


**Figure 2.** The average post-fission TKE measured for the  $^{235}\text{U}(n,f)$  reaction as a function of neutron energy.

In Figure 2, we show the mean post-fission TKE release for the fast neutron induced fission of  $^{235}\text{U}$  for the

energy range from 3.0 to 89.7 MeV. As observed for  $^{232}\text{Th}(n,f)$ , the mean TKE values decrease non-linearly with increasing neutron energy. A polynomial fit was made to these data. The resulting polynomial is  $\text{TKE}_{post} \text{ (MeV)} = 170.92 - 3.73 \log_{10} E_n - 0.65 (\log_{10} E_n)^2$ .

#### 3.3 $^{237}\text{Np}(n,f)$

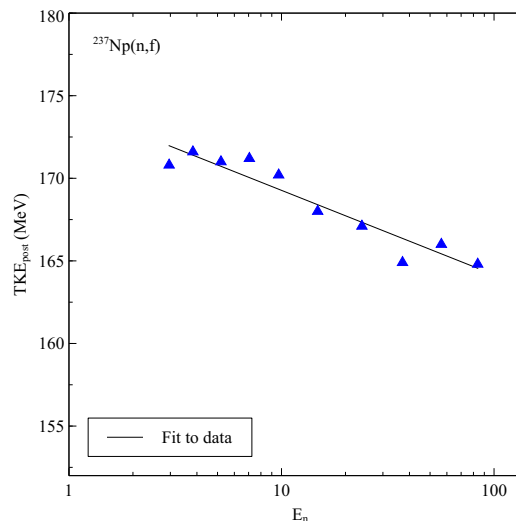


**Figure 3.** The average post-fission TKE measured for the  $^{237}\text{Np}(n,f)$  reaction as a function of neutron energy.

In Figure 3, we show the mean post-fission TKE release for the fast neutron induced fission of  $^{237}\text{Np}$  for the energy range from 2.4 to 83.8 MeV. As observed for  $^{232}\text{Th}(n,f)$ , the mean TKE values decrease non-linearly with increasing neutron energy. A polynomial fit was made to these data. The resulting polynomial is  $\text{TKE}_{post} \text{ (MeV)} = 174.38 - 5.11 \log_{10} E_n$  for  $E_n > 1$  MeV.

It is clear from Figures 1-3 that the post-neutron emission TKE plots for the three systems we have studied are similar apart from a shift in the TKE values with increasing  $Z$  and  $A$  of the fissioning systems. The data from Figures 1-3 and similar plots for other fissioning systems can be used to reliably predict the TKE values in fast neutron induced fission.

#### 3.4 TKE distribution variances

Another interesting feature of the TKE distributions is the variances of the TKE distributions. In Figures 4-6 we show the variances of the TKE distributions for the fast neutron induced fission of  $^{232}\text{Th}$  (Fig. 4),  $^{235}\text{U}$  (Fig. 5) and  $^{237}\text{Np}$  (Fig. 6). What is striking about these distributions is that the variances become smaller as the  $Z, A$  of the fission system increases. While there is some ‘spatter’ in the data, this trend seems clear and is not expected in a simple model of fission

#### 3.5 Models for the TKE release in fission.

To understand the data we have discussed up to this point, it is useful to compare our observations with predictions

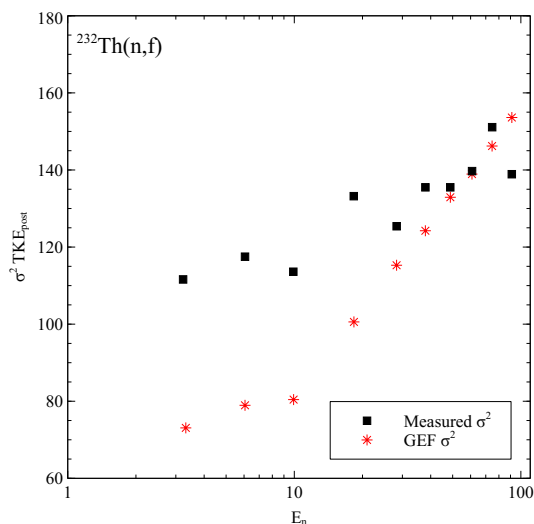


**Figure 4.** Measured and GEF calculated variances of the TKE distributions for the fast neutron induced fission of  $^{232}\text{Th}$ .

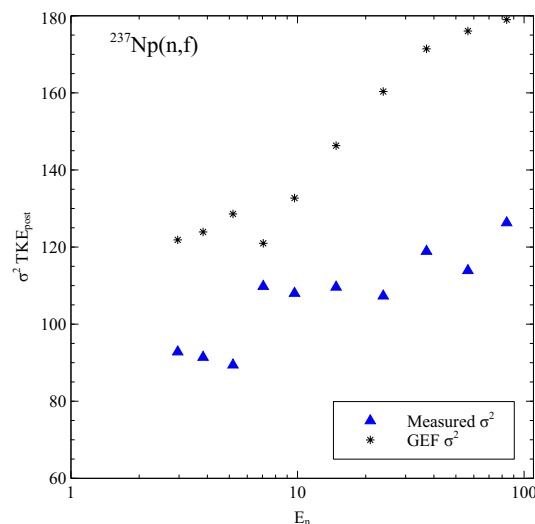


**Figure 6.** Measured and GEF calculated variances of the TKE distributions for the fast neutron induced fission of  $^{237}\text{Np}$ .

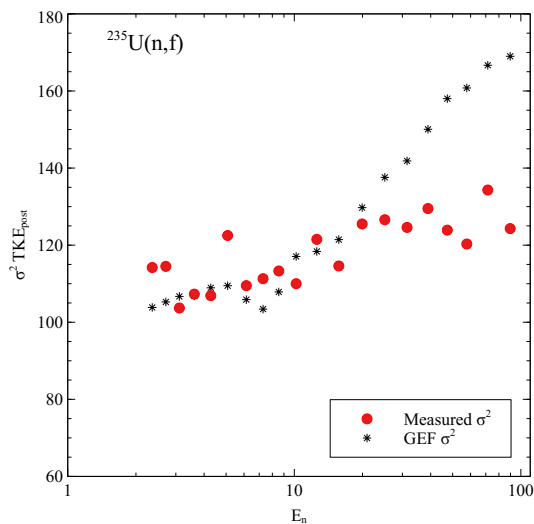


**Figure 5.** Measured and GEF calculated variances of the TKE distributions for the fast neutron induced fission of  $^{235}\text{U}$ .

(not “post-dictions”) of these quantities. One such prediction of the observables in fast neutron induced fission is the general description of fission observables (**GEF**), which is a semi-empirical model for the calculation of fission observables, with 50 adjustable parameters. The version of the code used in this study is GEF 2019/1.3, downloaded May 2019 [7]. The main ingredients of the GEF model are:

- (a) The mass division and the charge distribution are calculated assuming a statistical population of states in the fission valleys at freeze-out. The freeze-out time considers the influence of fission dynamics and is not the same for different collective variables.
- (b) The compound nucleus and fission fragment properties are assumed to be separable.
- (c) Five fission channels are considered. The strengths of the shells in the fission valleys are identical for all

fissioning systems. The mean positions of the heavy fragments in the asymmetric fission channels are essentially constant in atomic number.

(d) The stiffness of the macroscopic potential with respect to mass asymmetry is deduced from the widths of the measured mass distributions.

(e) An excitation energy sorting mechanism determines the prompt neutron yields and the odd-even effect in fission fragment yields of even  $Z$  and odd  $Z$  systems.

(f) Neutron evaporation is calculated with a Monte Carlo statistical code using level densities from empirical systematics and binding energies with theoretical shell effects with gamma competition included.

A notable aspect of the GEF code is that it postulates that as  $E^*$  increases, the excess energy goes to the heavy fragment only.

In Figures 7-9, we show the measured TKE distributions from this work and the predictions of the GEF model. For the  $^{235}\text{U}(n,f)$  reaction, there is good agreement between the GEF predictions and the measured data. For the  $^{232}\text{Th}(n,f)$  reaction, the agreement between the GEF predictions and the data is not good. For the  $^{237}\text{Np}(n,f)$  reaction, the agreement between the predicted and measured values of the TKE is abysmal. It is puzzling to us as to why a “50 parameter model” such as GEF does not do a better job of accounting for the measured data.

## 4 Summary and Conclusions

We have presented measurements of the TKE release in the fast neutron induced fission of the actinide nuclei,  $^{232}\text{Th}$ ,  $^{235}\text{U}$  and  $^{237}\text{Np}$ . Our measured values of the TKE release are in good agreement with the semi-empirical GEF model for the case of  $^{235}\text{U}(n,f)$  but not for  $^{237}\text{Np}$  or  $^{232}\text{Th}$ . In addition, we find the variances of the TKE distributions become smaller as the  $Z,A$  of the fissioning system increase, an unexpected finding.

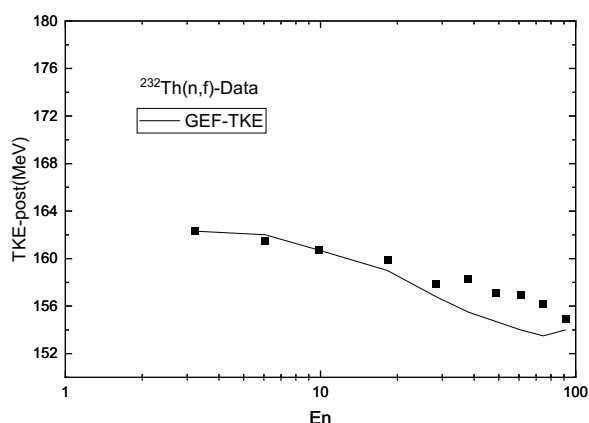


**Figure 7.** A comparison between the measured values of the TKE and those predicted by the GEF model for the fast neutron induced fission of  $^{232}\text{Th}$ .

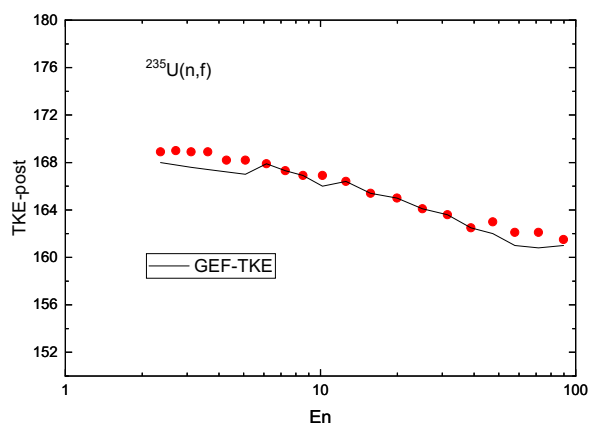


**Figure 8.** A comparison between the measured values of the TKE and those predicted by the GEF model for the fast neutron induced fission of  $^{235}\text{U}$ .

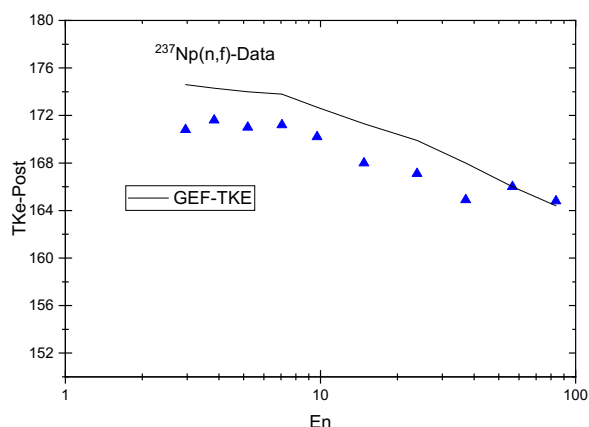


**Figure 9.** A comparison between the measured values of the TKE and those predicted by the GEF model for the fast neutron induced fission of  $^{237}\text{Np}$ .

## Acknowledgments

We gratefully acknowledge the financial support of the U.S. Dept. of Energy, NNSA, under grant DE-NA0022926 and the U.S. Dept. of Energy, Office of Science, Nuclear Physics Division, under grant DE-FG06-97ER41026.

## References

- [1] J. King, R. Yanez, W. Loveland, J.S. Barrett, B. Oscar, N. Fotiadis, F. Tovesson, and H.Y. Lee, *Eur. Phys. J. A* **53**, 238 (2017).
- [2] R. Yanez, J. King, J.S. Barrett, W. Loveland, N. Fotiadis and H.Y. Lee, *Nucl. Phys. A* **970**, 65 (2018).
- [3] A. Pica, A.T. Chemey, L. Yao, W. Loveland, H.Y. Lee and S. A. Kuvin, *Phys. Rev. C* **102**, 064612 (2020).
- [4] M.J. Silveira, A. Pica and W. Loveland, *Nucl. Instru. Methods Phys. Res. Sect. A* **982**, 164750 (2020)
- [5] H.W. Schmitt, J.H. Neiler and F.J. Walter, *Phys. Rev* **141**, 1146 (1966).
- [6] L.C. Northcliffe, and R. Schilling, *At. Data Nucl. Data Tables* **7**, 233 (1970).
- [7] K.H. Schmidt, B. Jurado, C. Amouroux, and C. Schmitt, *Nuclear Data Sheets* **131**, 107 (2016).
- [8] M.J. Bennett and W.E. Stein, *Phys. Rev.* **156**, 1277 (1967)
- [9] G.F. Bertsch, W. Loveland, W. Nazarewicz. and P. Talou, *J. Phys. G. Nucl. Part. Phys.* **42**, 077001 (2015).